Conference 2
10 September 2008

Conference Coordinator:
Todd M. Bell, DVM,

Wednesday Slide Conference

Moderator:

Dr. Sarah Hale, DVM, Diplomate ACVP

CASE I – CRL 2008-1 (AFIP 3104062)

Signalment: Mouse (Mus musculus), strain unknown (homozygous for foxn1^{nu}), age and gender unknown.

History: Submitted to necropsy for evaluation of scaly skin.

Gross pathologic findings: Skin over the entire body surface is hyperkeratotic, with white flakes.

Laboratory results: PCR of skin surface swabs positive for *Corynebacterium bovis*.

Histopathologic description: Skin (nude): The epidermis is diffusely acanthotic, approximately 3-fold thicker than normal. Abundant keratinaceous debris covers the surface (diffuse orthokeratotic hyperkeratosis) (Fig. 1-1). Numerous colonies of small bacteria mix with hair and keratinaceous debris on the surface of the hyperkeratotic layer (Fig. 1-2). The bacteria appear coccoid in some areas, and as short bacilli in irregular

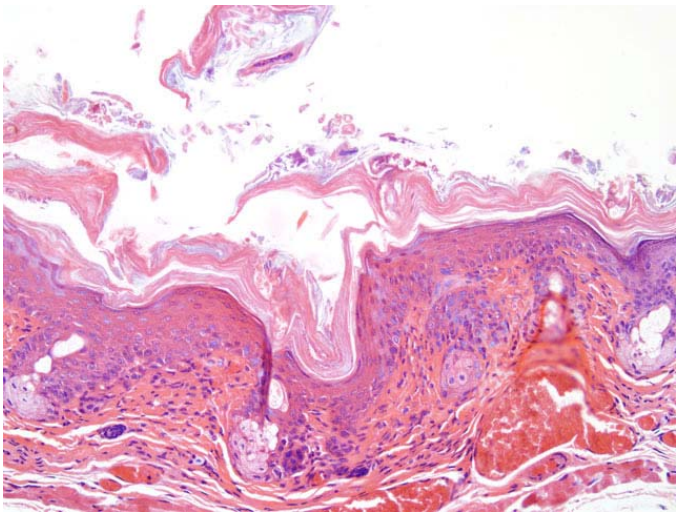

1-1 Haired skin, mouse. Diffusely there is epidermal hyperplasia with orthokeratotic hyperkeratosis and there are scattered lymphocytes, plasma cells, histiocytes and fewer neutrophils within the superficial dermis. (HE 200X).

* Sponsored by the American Veterinary Medical Association, the American College of Veterinary Pathologists and the C. L. Davis Foundation.

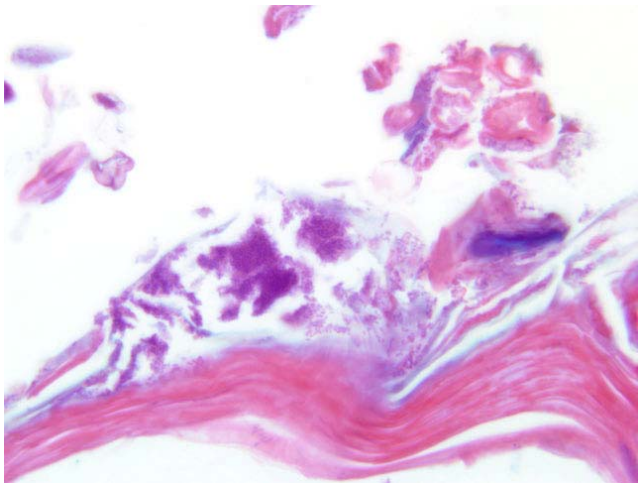

1-2 Haired skin, mouse. Within the stratum corneum there are few small colonies of approximately 1 micron diameter bacilli. (HE 600X).

---

branching clusters in a few others. The dermis is diffusely mildly infiltrated by mononuclear leukocytes and a few neutrophils. Mast cells are prominent.

Brown and Brenn Gram's stain: The bacteria are Gram positive. The predominant type is short coryneforms, arranged in typical corynebacterial arrays.

Contributor's morphologic diagnosis: Dermatitis, subacute, diffuse, mild, with prominent acanthosis, hyperkeratosis and coryneform bacteria.

Contributor's Comment: Corynebacterial hyperkeratosis, the so-called "scaly skin disease", remains fairly common, with approximately 2% of nude mice submitted to our diagnostic laboratory from non-vendor sources being confirmed with the disease.

Corynebacterial hyperkeratosis has been recognized for decades in athymic nude mice, but also occurs in SCID mice and can be experimentally reproduced in euthymic hairless mice.(1). Morbidity varies, but can be high. Mortality is usually very low except in suckling mice, which can have high mortality. Immunocompetent mice, other than hairless strains, may have asymptomatic infection, but evidence suggests that infection is cleared in these mice.(2,3)

Clinical signs include hyperkeratosis, decreased activity and a wrinkled appearance which probably indicates dehydration. Signs typically appear in susceptible mice about one week after exposure, persist for a week or more, and then usually disappear. Microscopically, the acanthosis remains after the hyperkeratosis resolves; the infection also persists. The mechanism by which *C. bovis*, a lipophilic bacterium which colonizes the stratum corneum, causes acanthosis and hyperkeratosis is unknown, as is the reason for resolution of the hyperkeratosis.

Histologic features of this case are typical. Hyperkeratosis can be difficult to assess microscopically, is transitory in this disease, and is non-specific; it may be caused by various conditions. Thus, greater diagnostic significance should be given to the acanthosis. Diffuse acanthosis, with a mild non- suppurative dermatitis and the presence of Gram positive coryneform bacteria in the stratum corneum is sufficient for a diagnosis, although in most situations confirmation by culture and or PCR is preferred(4). Other corynebacteria may also colonize the skin surface; our laboratory has identified *C. jeikeium*, *C. minutissimum* and Group F2. The latter two organisms are now included in *C. amycolatum*. None of these are thought to cause skin disease in mice.

In addition to mortality in suckling immunodeficient mice, *C. bovis* has been reported to slow xenograft growth and increase toxicity observed after chemotherapeutic agents. The mechanism of this is unknown, but the contributor speculates that it might be related to dehydration (symptomatic mice virtually always appear markedly dehydrated, conceivably due to alterations in epidermal barrier function from the diffuse skin disease). Retarded xenograft growth could also possibly be due to non-specific stimulation of host defense mechanisms such as NK cell activity. Non-specific antitumor effects have previously been described for *C. kutscheri*.(6)

Control of *C. bovis* infection is difficult. The bacterium is readily transmitted by fomites and is resistant to drying. Our diagnostic laboratory has found positive PCR samples on swabs from cage exteriors, door knobs and even tumor lines passaged as tumor fragments.

AFIP Morphologic Diagnosis: Skin: Hyperkeratosis, orthokeratotic, diffuse, moderate, with epidermal hyperplasia and mild subacute dermatitis.

Conference Comment: The contributor did an excellent job of summarizing the clinical manifestations, strains affected, and histologic features of *Corynebacterium bovis* infections in mice. This comment will briefly touch on the gross and histologic features of *Corynebacterium kutscheri*, another important organism

in laboratory animals.

Mice and Rats: *Corynebacterium kutscheri* is a Gram-positive, diphtheroid bacillus that is the cause of "pseudotuberculosis" in both mice and rats. The normal route of entry of *C. kutscheri* is through the oral or gastrointestinal mucosa with subsequent hematogenous spread throughout the body. An immunosuppressive event usually precedes clinical disease.(5)

Common gross findings include suppurative bronchopneumonia with randomly distributed caseopurulent nodules; raised, multifocal to coalescing caseopurulent nodules in the heart, liver, or kidney; reactive hyperplasia in lymph nodes near an active site of infection; and pedal arthritis.(5)

On histological section, the bacteria form large colonies surrounded by abundant neutrophils and necrotic debris. Because the disease spreads via sepsis, the suppurative lesions in the lung are randomly distributed. This is an important distinguishing feature between this disease and the disease caused by *Mycoplasma pulmonis*, which is closely associated with the airways and causes bronchiectasis. The large bacterial colonies of *C. kutscheri* are pathognomonic and are described as resembling Chinese letters. Interstitial pneumonia is also commonly present in association with *C. kutscheri* infection and is characterized by hypercellular alveolar septa and pulmonary edema.(5)

Hamsters: These rodents are considered carriers of *C. kutscheri* but are typically resistant to systemic disease. (5)

Contributing institution: Charles River; www.criver.com

References:

1. Clifford CB, Walton BJ, Reed TH, Coyle MB, White WJ, Amyx HL: Hyperkeratosis in nude mice caused by a coryneform bacterium: Microbiology, transmission, clinical signs, and pathology. Lab Anim Sci 1995, 45:131-139
2. Gobbi A, Crippa L, Scanziani E: Corynebacterium bovis infection in immunocompetent hirsute mice [see comments]. Lab Anim Sci 1999, 49:209-211
3. Gobbi A, Crippa L, Scanziani E: Corynebacterium bovis infection in waltzing mice [letter; comment]. Lab Anim Sci 1999, 49:132-133
4. Kita E, Nishikawa F, Yagyu Y, Hamuro A, Oku D, Emoto M, Katsui N, Tanikawa I, Kashiba S: Nonspecific stimulation of host defense by Corynebacterium kutscheri. I. Antitumor effect. Nat Immun Cell Growth Regul 1989, 8:313-324
5. Percy DH, Barthold SW: Pathology of Laboratory Rodents and Rabbits, 3rd ed., pp. 72, 147-148, 192. Blackwell Publishing, Ames, Iowa, 2007
6.Russell, S, Riley, LK, Maddy, A, Clifford, CB, Russell, RJ, Franklin, CL, Hook, RR, and Besch-Williford, CL Identification of Corynebacterium bovis as the etiologic agent of hyperkeratosis in nude mice and development of a diagnostic polymerase chain reaction assay. Laboratory Animal Science 48 [4], 412. 1998 Ref Type: Abstract

CASE II - 07-276-3 (AFIP 3102251)

Signalment: 10-month-old female C57BL/6 mouse (*Mus sp.*) #202, with homozygous point mutation in *Mcm4* gene (*Mcm4*$^{Chaos3/Chaos3}$).

History: The mouse was euthanized after developing an enlarged abdomen and lethargy.

Gross pathologic findings: The liver was pale brown, markedly enlarged and had rounded edges. The spleen was diffusely enlarged and also had rounded edges.

Histopathologic description: Liver is diffusely hypercellular and the capsular surface has slightly irregular contour. Normal hepatic architecture is disrupted by filling of multifocal sinusoids and veins with small to moderate numbers of neoplastic cells arranged individually and in small clusters (Fig 2-1). The neoplastic cells are moderately sized (2x smaller than hepatocytes), round to oval or elongate, with distinct cytoplasmic margins and moderate amount of eosinophilic cytoplasm that occasionally contains moderate amount of green-yellow pigment (hemosiderin). Occasionally, there are RBCs within neoplastic cell cytoplasm (erythrophagocytosis). The nucleus is round to oval, often eccentrically placed and with coarsely clumped chromatin and indistinct nucleolus. There is mild anisocytosis and anisokaryosis and rare mitotic figures and binucleated cells. Other changes in the liver that are present to variable degree in submitted slides include a few small foci of hepatic lipidosis, occasional dilatation of sinusoids, rare foci of extramedullary hematopoiesis containing erythroid and granulocyte precursors and low numbers of megakaryocytes, presence of eosinophilic globular

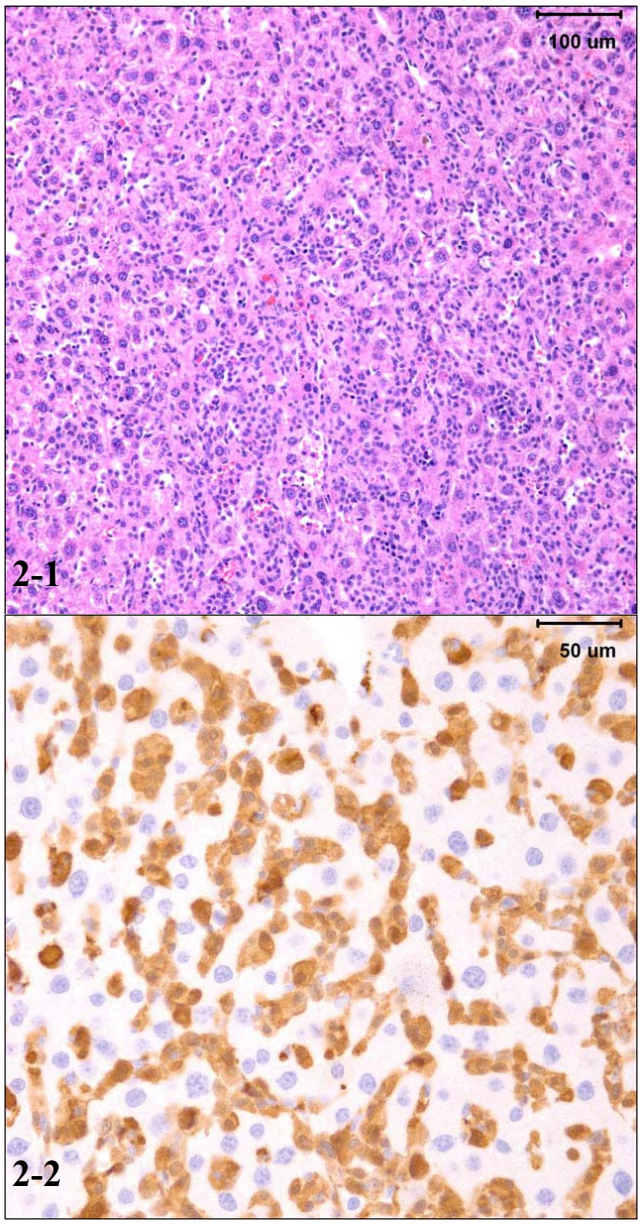

2-1 Liver, mouse. Diffusely infiltrating and expanding the sinusoids are high numbers of round cells.
2-2 Liver, mouse. Diffusely neoplastic cells are show strong cytoplasmic immunopositivity for Mac-2.

Photomicrographs courtesy of Veterinary Population Medicine Department, College of Veterinary Medicine, University of Minnesota. DAB with hematoxylin counter-stain.

intracytoplasmic inclusions in some hepatocytes and occasional hepatocytes filled with moderate amount green-brown granular pigment.

Laboratory results: Immunohistochemistry for macrophage marker Mac-2 was done using M3/38 antibody clone from Cedarlanes. The cytoplasm of intrasinusoidal neoplastic round cells was strongly positive for Mac-2 (Fig 2-2).

Contributor's morphologic diagnosis: Liver: Histiocytic sarcoma.
Spleen (tissue not included): Erythroid hyperplasia, diffuse, marked.

Contributor's Comment: Histiocytic sarcoma (HS) in mice arises from the cells of mononuclear phagocytic system and most commonly affects liver and uterus with less frequent involvement of spleen, lung, lymph node, ovary, kidney and bone marrow.(3, 8) The incidence is dependent on strain, sex, age, nutrition, and varies from study to study .(2, 4) For example, HS incidence in C57BL/6 mice is higher than in most other strains of inbred mice, and the disease in this strain occurs rarely before 12 months of age.(2, 3, 4) One of the highest incidences of HS has been reported by Blackwell in a study that determined effect of dietary restriction on the incidence of tumors in C57BL/6 mice.(2) HS was the most prevalent neoplasm in this study that involved almost 1000 mice over period of 3 years. Overall lifetime incidence of HS was ~30% in *ad lib itum* fed C57BL/6 female mice in comparison with ~ 55% in similarly fed male mice. 40% reduction in the feed resulted in slightly decreased incidence of HS in male mice and increased HS incidence in female mice to 50%.

The gross and microscopic appearance of HS depends on organs involved. The liver involvement is the most common manifestation of HS regardless of the mouse strain.7 The liver with HS is severely, diffusely enlarged and without focal lesions. Histologically, tumor cells are present diffusely or multifocally with in sinusoids and vascular spaces. Progressive growth of neoplastic cells leads to compression of hepatic cords and hepatocyte atrophy.(3, 7) Uterine involvement is strong ly strain-dependent in mice: uterine HS is rare in C57BL/6 mice but common in CBA mice.(7) HS in uterus may present as diffuse thickening of both horns or as 1 to several variably sized nodules. Histologically, neoplastic histiocytic cells that infiltrate uterine wall tend to be elongated to fusiform.(3, 7) Erythrophagocytosis may

be associated with the neoplastic infiltrates, particularly in the liver and multinucleated giant cells may be present in some tumors.(3, 7) Immunohistochemical stains that aid identification of neoplastic cells as histiocytes include Mac-2, F4/80, and lysozyme.(9)

Recent publications have linked development of HS in the liver in C57BL6/J mice with concurrent hepatic (but not splenic) extramedullary hematopoiesis (EMH) and hematologic abnormalities such as anemia.(1, 5) At this point it is not clear whether HS and hepatic EMH are co-incidental lesions or if one of them leads to the other. Concurrent hematologic abnormalities may suggest genetic abnormality in myeloid stem cells.

The submitted case is from a mouse with homozygous, single base mutation in *Mcm4* gene known as Chaos3. This mutation induced high incidence of mammary adenocarcinomas in C3H mice.(7) In contrast, C57BL/6 mice with Chaos3 mutation have high prevalence of histiocytic sarcoma with shortened tumor latency of less than 12 months. Diffuse liver involvement is noted most commonly in these mice but nodular tumor infiltrates and marked destruction of hepatic parenchyma by HS is seen occasionally. All mice with hepatic HS have extramedullary hematopoiesis in the liver and marked erythroid hyperplasia in the spleen. Some mice have intraabdominal solid masses in peripancreatic omentum and elsewhere diagnosed as HS based on presence of Mac-2 positive cells with histiocytic appearance (spindle to polygonal cells, abundant cytoplasm, and oval to indented nucleus) and neoplastic features (moderate mitotic figure rate and bizarre mitoses).

Gene complex *MCM2-7* which includes *MCM4* encodes protein complex that is recruited to DNA replication origins and ensures a single initiation of DNA synthesis during S phase restricting genome replication to once per cell cycle.(7) Chaos3 mutation was first identified in the screen for chromosome instability. High incidence of tumors and short tumor latency periods in mice with *Mcm4Chaos3/Chaos3* suggests that genomic instability may have a causative role in cancer. It is not clear at this point yet whether C57BL/6 mice with *Mcm4Chaos3/Chaos3* genotype have hematologic abnormalities such as anemia concurrently with HS.

AFIP Morphologic Diagnosis: 1. Liver: Histiocytic sarcoma.
2. Liver, hepatocytes: Microvesicular lipidosis, multifocal, moderate.

Conference Comment: The contributor provided a thorough overview of the gross and histologic lesions of histiocytic sarcoma in mice. This brief discussion will focus on **histiocytic sarcoma in rats.**

In rats, the most commonly affected strain is Sprague – Dawley, and tumors are generally seen in animals over 12 months of age with no gender preference. The organs affected in rats are similar to those in mice; the most common sites are liver, lymph nodes, spleen, mediastinum, retroperitoneum, and subcutaneous tissue. Affected rats most commonly have nodules of tumor cells that displace normal organ parenchyma, whereas in the mouse liver, neoplastic cells typically in filtrate sinusoids with no distinct mass formation.(6)

Histologically, tumor cells are pleomorphic with vesicular nuclei, prominent nucleoli, and abundant cytoplasm. Multinucleate giant cells are a common component of tumors with a predominantly histiocytic makeup. Because of the variable morphology of neoplastic histiocytes, the differential diagnostic list includes various sarcomas, lymphoma and granulomatous inflammation.(6)

Contributing institution: Veterinary Population Medicine Department, College of Veterinary Medicine, University of Minnesota.

References:
1. Barker JE, Deveau SA, Compton ST, Fancher K, Eppig JT: High incidence, early onset of histiocytic sarcomas in mice with Hertwig's anemia. Exper. Hematol. **33**: 1118-2911, 2005
2. Blackwell BN, Bucci TJ, Hart RW, Turturro A: Longevity, body weight, and neoplasia in *ad libitum*-fed and diet-restricted C57BL6 mice fed NIH-31 open formula diet. Toxicol. Pathol. **23**: 570-582, 1995
3. Frith CH: Histiocytic sarcoma, mouse. In: Monographs on Pathology of Laboratory Animals. Hematopoietic system, Jones TC, Ward JM, Mohr U, Hunt RD (eds). Springer-Verlag, Berlin, Heidelberg, pp 58-65, 1990
4. Frith CH, Ward JM, Chandra M: The morphology, immunohistochemistry and incidence of hematopoietic neoplasms in mice and rats. Toxicol. Pathol. **21**: 206-218, 1993
5. Lacroix-Triki M, Lacoste- Collin L, Jozan S, Charlet JP, Caratero C, Courtade M: Histiocytic sarcoma in C57BL/6J mice is associated with liver hematopoiesis: Review of 41 cases. Toxicol. Pathol. **31**: 304-309, 2003
6. Percy DH, Barthold SW: Pathology of Laboratory Rodents and Rabbits, 3rd ed., pg. 116, 170-171, 172. Blackwell Publishing, Ames, Iowa, 2007
7. Shima N, Alcaraz A, Liachko I, Buske TR, Andrews CA, Munroe RJ, Hartford SA, Tye BK, Schimenti JC: A

viable allele of Mcm4 causes chromosome instability and mammary ade nocarcinomas in m ice. Nature Genetics **39**: 93-98, 2007
8. Turu sov VS: Histio cytic sarcoma. IARC Sci. Pub l. **111:** 671-680, 1994
9. War d JM, Shel don W : Ex pression of mononuclear phagocyte an tigens in histiocytic sarco ma of m ice. Vet. Path. **30**: 560-565, 1993

CASE III – 08014 (AFIP 3103042)

Signalment: 27-year-old, male, cy nomolgus m acaque (Macaca fascicularis), nonhuman primate

History: This animal arrived at Wake Forest University from Ind onesia ab out 9 y ears before de ath. It was diagnosed with type 2 diabetes on 3/6/2008 (glucose 328 g/dL), and on the following day, became lethargic and dehydrated. In sulin t reatment and su pportive fl uid therapy were attempted, but the animal died on 3/9/2008.

Gross pathologic findin gs: The major gross lesion was in th e lun g. Th e en tire left lu ng was four ti mes larg er than normal, firm, an d tan to yello wish-brown, with adherence to the body wall in some areas (Fig. 3-1, 3-2). Similar ch anges were present in th e m iddle righ t lun g lobe. Cut s urfaces revealed suppurative exudate (Fig. 3-3), and 10-20% of the parenchyma was replaced by dense fibrous connective tissue.

Case III.
Laboratory results:

Serum chemistry:
Glucose, 348 mg/dL
BUN 29 mg/dL
K^+ 6.2 mEq/L
Alkaline phosphatase 588 µ/L
Cholesterol 1099 mg/dL

Hematology:
CBC:
RBC, 6.77 x 10^5/µL
Hematocrit, 42.3 %
Hemoglobin, 12 mg/dL
MCV, 62fl
MCHC 28.4 g/dL
Platelets 181 x 10^3/µL
WBC 15.9 x 10^3/µL
Neutrophils, 77% (12243)
Bands, 0
Lymphocytes 17% (2703)
Monocytes, 5% (795)
Eosinophils, 1% (159)
Basophils, 0

In addition to the pulmonary lesion, the coronary arteries were seg mentally th ickened b y yello w plaques on th e intimal surfaces (atherosclerosis).

Microbiology:
Pleural fluid and a lung sw ab were submitted for bacterial cu lture. A heavy pu re growth (4 +) of *Corynebacterium ulcerans* was recovered.

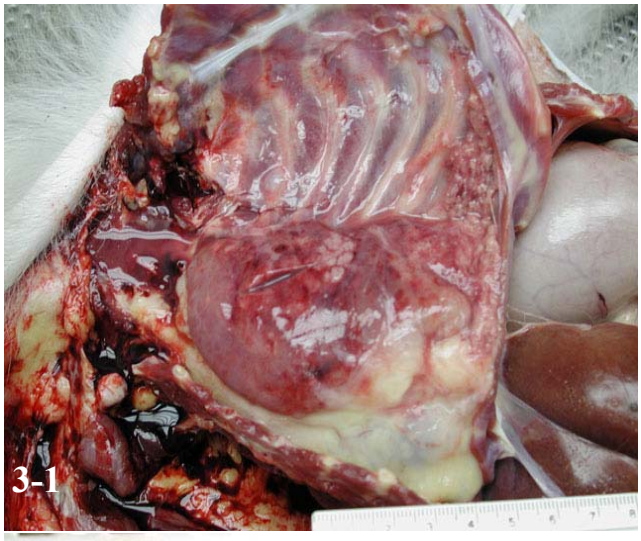

3-1. Lung, Cynomolgus macaque. Suppurative pleuropneumonia.
3-2. Lung, Cynomolgus macaque. Necrosuppurative pleuropneumonia with lymphadenitis and mediastinal edema.

Gross photographs courtesy of Animal Resources Program, Wake Forest University Health Sciences, Winston-Salem, North Carolina.

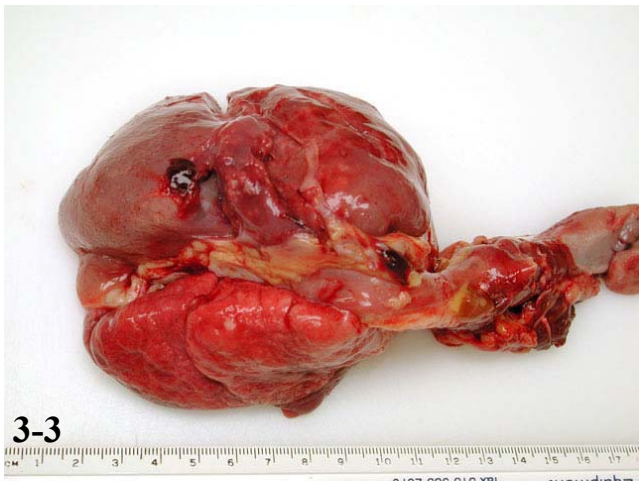

3-3. Lung, Cynomolgus macaque. Necrosuppurative pleuropneumonia with intralobular edema and hemorrhage. Gross photograph courtesy of Animal Resources Program, Wake Forest University Health Sciences, Winston-Salem, North Carolina.

3-4 Lung, Cynomolgus macaque. The normal lung architecture is lost and there are large coalescing areas of lytic necrosis admixed with a cellular infiltrate. (HE 40X).
3-5 Lung, Cynomolgus macaque. Normal lung parenchyma is necrotic and replaced by fibrin admixed with cellular and karyorrhectic debris. (HE 200X).
3-6 Lung, Cynomolgus macaque. Scattered throughout the areas of necrosis there are large colonies of 1-2 micron diameter bacilli. (HE 400X).

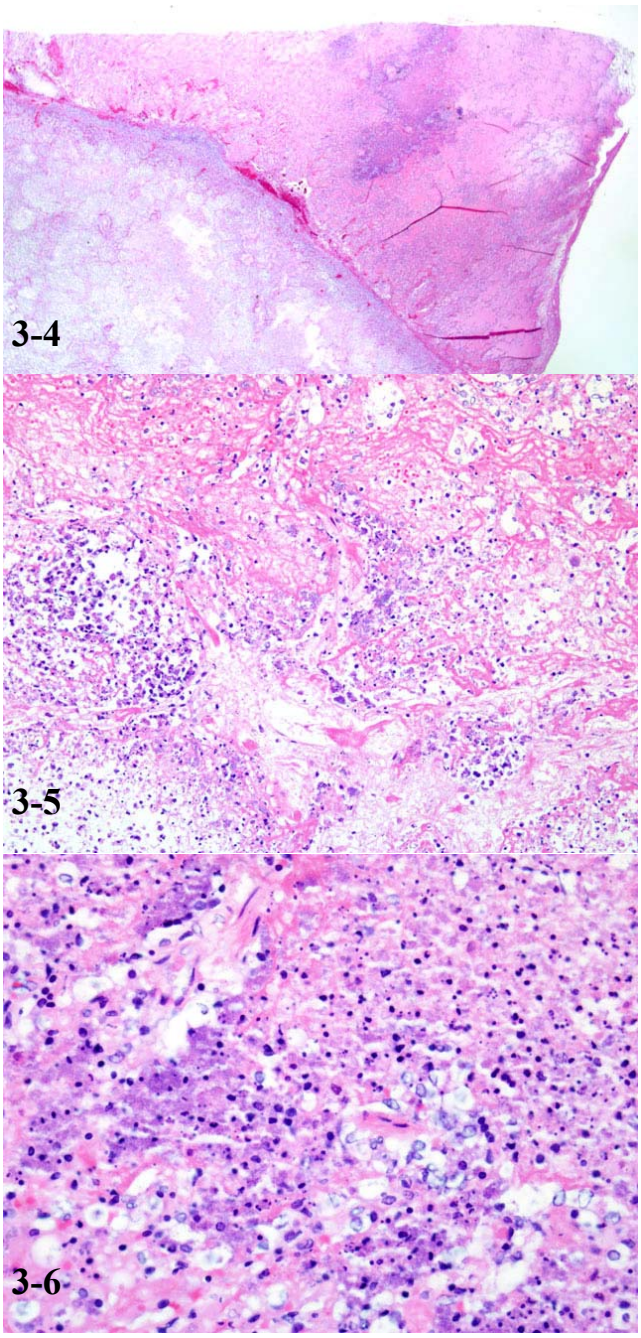

Histopathologic description: Lung: The pulmonary architecture is extensively distorted (Fig. 3-4) by a necrotizing inflammatory reaction composed of abundant neutrophils and protein-rich edema fluid, which fills alveoli and bronchioles. Alveolar walls are often effaced (Fig. 3-5) and bronchiolar epithelium is often absent. Pale perivascular spaces measuring up to 500um in width contain fibrin and edema fluid. Vessels are variably infiltrated by neutrophils and mononuclear phagocytes, contain thrombi, and are surrounded by myriads of short bacterial rods. Similar bacterial colonies are also scattered throughout the pulmonary parenchyma and subpleural space (Fig. 3-6). The pleura is thickened up to 1.5mm owing to the presence of variably mature fibrous connective tissue and suppurative inflammation. Gram staining demonstrates mats of pleomorphic Gram positive bacilli throughout the lung.

Contributor's morphologic diagnosis: Pneumonia, diffuse, chronic, severe, fibrinosuppurative with intralesional bacteria
(Etiology: *Corynebacterium ulcerans*)

Contributor's Comment: Corynebacteria are Gram positive, non-motile, pleomorphic bacilli.(2) Corynebacterium ulcerans was first isolated in 1926 from a human throat lesion[4], and has since been considered a common cause of laryngitis and cutaneous granulomas in humans.(2) It has also been isolated from abscesses and

causes pneumonia and mastitis in nonhuman primates.(3) It is considered a commensal of horses and cattle, although it can cause mastitis and cutaneous infections in cattle (5), and is widely distributed in soil and water. It is often isolated from non-pasteurized milk, the drinking of which has been linked to human infections.(6) Fatal pneumonia caused by C. ulcerans has been reported in humans and macaques.(2) A retrospective study of respiratory disease in 272 nonhuman primates (75 cynomolgus macaques, 97 rhesus macaques, 100 vervets) indicated that C. ulcerans and Streptococcus pneumoniae were major causes of winter respiratory infections in cynomolgus macaques.(3)

The pathogenicity of C. ulcerans is facilitated by potent exotoxins, including diphtheria toxin which inhibits protein synthesis, as well as necrotizing toxin which increases vascular permeability resulting in edema. After inhalation, C. ulcerans proliferates in the respiratory tract epithelium. Subsequent release of the exotoxins causes epithelial necrosis, which in turn initiates marked interstitial edema, neutrophil infiltration, and fibrinosuppurative exudation.(1)

The differential diagnosis for fibrinosuppurative bronchopneumonia in cynomolgus macaques should include Streptococcus pneumoniae, Pasteurella spp., Nocardia spp., Actinobacillus spp., Klebsiella spp., and Legionella pneumophila as well as Corynebacterium sp.

AFIP Morphologic Diagnosis: Lung: Pleuropneumonia, fibrinonecrotic, diffuse, severe, with abundant coccobacilli.

Conference Comment: Genetic analysis has revealed that *Corynebacaterium ulcerans* is a unique organism that is very closely related to *Corynebacterium diptheriae* and *Corynebacterium pseudotuberculosis*.(1)

Corynebacterium ulcerans can produce diphtheria toxin similar to that of *C. diphtheriae*. *C. diphtheriae* produces a phage-encoded A-B toxin that blocks protein synthesis. Even after vaccination with diphtheroid toxin, *C. diphtheriae* can still colonize the epithelium, and the vaccine does protect people from the harmful effects of the toxin. Release of the exotoxin in unvaccinated individuals causes necrosis of the epithelium and subsequent profuse fibrionsuppurative exudation. The settling of this exudate on the already ulcerated epithelial surface results in formation of the firm diphtheritic membrane characteristic of the disease. If the fulminant infection is stopped, the membrane may be sloughed via coughing or enzymatic digestion, and the patient can recover.(4)

Contributing institution: Animal Resources Program, Wake Forest University Health Sciences, Winston-Salem, NC; http://www1.wfubmc.edu/pathology/training/index.htm

References:

1 AFIP Wednesday slide conference 23 case # 3, 1999 http://www.afip.org/vetpath/WSC/wsc99/99wsc23.htm
2. Dessau RB, Brandtchristensen M, Jensen OJ, Tonnesen P: pulmonary nodules due to corynebacterium ulcerans. European Respiratory Journal 8: 651-653, 1995
3. Panaitescu M, Maximescu P, Michel J, Potorac E: Respiratory pathogens in non-human primates with special reference to Corynebacterium ulcerans. Lab Animal 11:155-157, 1977
4. Mc Adam AJ, Sharpe AH: Infectious Diseases. In Robins and Cotran Pathologic Basis of Disease, ed. Kumar V, Abbas AK, Fausto N, 7th ed., pp. 374, Elsevier Saunders, Philadelphia, PA 2005
5. Sing A, Hogardt M, Bierschenk S, Heesemann E: Detection of differences in the nucleotide and amino acid sequences of diphtheria toxin from Corynebacterium diphtheriae and Corynebacterium ulcerans causing extrapharyngeal infections. Journal of Clinical Microbiology 41: 4848-4851, 2003
6. Wagner J, Ignatius R, Voss S, Hopfner V, Ehlers S, Funke G, Weber U, Hahn H: Infection of the skin caused by Corynebacterium ulcerans and mimicking classical cutaneous diphtheria. Clinical Infectious Diseases 33: 1598-1600

CASE IV –08012 (AFIP 3103041)

Signalment: 7-year-old, female, African green monkey, *Chlorocebus aethiops*, non-human primate

History: The animal failed to recover from sedation for routine tuberculosis testing.

Gross pathologic findings: The animal was severely dehydrated and had multiple gastric ulcerations in the fundus. Both thyroid glands were unremarkable, each weighed 0.17 g and 0.23 g.

Histopathologic description: Mostly lymphocytes admixed with fewer plasma cells infiltrate the interstitium diffusely, with multifocal intensification, separating and sometimes sequestering the follicles (Fig.

Case IV. Laboratory results:

Test	Result	Humans Reference Range[6]
Total Thyroxine (TT4)	14	60-140 nmol/L
Total Triiodothyronine (TT3)	2.3	1.1-2.7 nmol/L
Free Thyroxine (FT4)	7	10-25 pmol/L
Free Triidothyronine (FT3)	6.8	3-8 pmol/L
T4 Autoantibody*	15%	N/A
T3 Autoantibody*	3%	N/A

N/A: Not Available
*: Autoantibodies to T3 and T4 are presented as the percentage of hormone binding relative to each antibody negative control

---

4-1). In some instances the lymphocytes form follicles with germinal center formation (not present in all slides). The thyroid follicles range from 60-150 microns in diameter, and are often devoid of colloid. The follicular epithelial cells range from cuboidal to tall columnar, and are multifocally hyperplastic, forming 3-4 stratified layers, or papillary projections into the lumina. Ten to twenty percent of them are slightly shrunken, hypereosinophilic, and have deeply basophilic nuclei with condensed chromatin (apoptosis). Regularly the follicular epithelial are separated from the basement membranes by clear spaces, despite being attached to one another along their lateral sides. Sometimes the lumina are filled with sloughed cells admixed with foamy macrophages and cellular debris enmeshed in amorphous, pale eosinophilic material (Fig. 4-2).

Contributor's morphologic diagnosis: Thyroiditis, diffuse, chronic, marked, lymphocytic, Thyroid Gland.

Contributor's Comment: Chronic lymphocytic thyroiditis in humans and non-human primates is commonly recognized as an autoimmune disorder with a poorly understood pathogenesis. Diagnoses are made based on a thyroid test panel, clinical signs, and histologic findings. Spontaneous thyroiditis has been reported in laboratory rats, obese strains of chickens, dogs, and a cynomolgus monkey.(2,3)

Two types of autoimmune thyroiditis are described in humans, Graves' disease and Hashimoto's thyroiditis, the latter being more frequent.(3,4,6,8) In Graves' disease, the inflammation is mild, while the thyroid glands are enlarged due to proliferation of thyrocytes, resulting in follicular hyperplasia and hypertrophy. Graves' disease accounts for 50-80% of hyperthyroidism cases in humans, and results from circulating IgG antibodies that bind to and activate the G-protein-coupled thyrotropin receptor. Clinical pathological findings include decreased serum thyrotropin, elevated serum triiodothyronine (T3) and thyroxine (T4), with an increased fraction of T3 relative to T4.(1,3,6)

In Hashimoto's thyroiditis, the lymphocytic infiltration is prominent, often with germinal center formation, causing enlargement of the thyroid glands and destruction of the thyroid follicles, leading to hypothyroidism. The pathogenesis of Hashimoto's thyroiditis involves a delayed hypersensitivity reaction to thyroid epitopes. Sensitization of autoreactive CD4 + T-helper cells to these initiates the immunologic events leading to thyrocyte death. The effector mechanisms include destruction of thyrocytes by CD8+ cytotoxic T cells by exocytosis of perforin/granzyme granules or engagement of the death receptor, overproduction of inflammatory cytokines by CD4+ T cells, and the binding of antithyroid antibodies (anti-TSH receptor, antithyroglobulin, and antithyroid peroxidase antibodies) followed by antibody-dependent cell-mediated cytotoxicity. Hypothyroidism usually develops gradually, although in some cases it may be preceded by transient thyrotoxicosis due to the disruption of thyroid follicles, with secondary release of

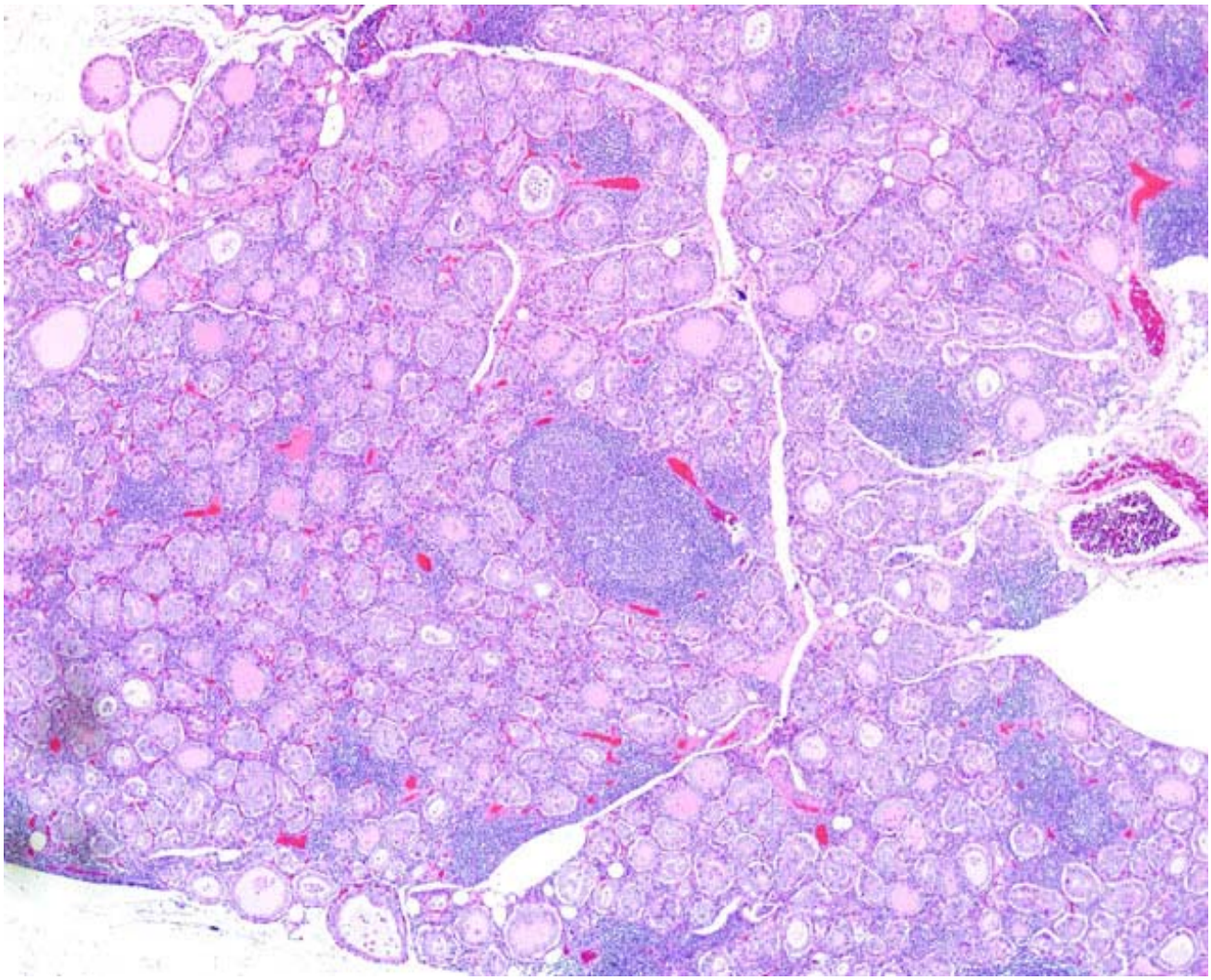

4-1 Thyroid gland, African green monkey. Multifocally, expanding the thyroid interstitium is a cellular infiltrate that often forms lymphoid follicles with vague germinal centers. (HE 40X).

---

thyroid hormones (hashitoxicosis).(2,3,6,8)

As there is relatively little literature on African green monkeys, normal reference ranges for humans (7) were used to confirm the presence of autoimmune thyroiditis in this case. Serum-binding assays to measure thyroxine (T4) and triiodothyronine (T3) autoantibodies revealed 15% and 3% more binding of the immunoglobulin to the T4 and T3, respectively, compare to each negative control. Low TT4 and FT4 support a diagnosis of hypothyroidism, which, combined with the histological appearance, resembles Hashimoto's thyroiditis in humans. Values of thyroid stimulating hormone (TSH), autoantibodies against thyroglobulin, thyroperoxidase, or TSH receptor are not available due to the limitation of serum available for testing.

AFIP Morphologic Diagnosis: Thyroid gland: Thyroiditis, lymphoplasmacytic, chronic, diffuse, marked, with follicular hyperplasia and colloid depletion.

Conference Comment: Other animal species with an autoimmune thyroiditis resembling Hashimoto's disease include dogs, obese strains of chickens, nonhuman primates, and Buffalo rats. The pathogenesis of autoimmune thyroiditis in the dog is not completely understood, but it seems to stem from production of autoantibodies directed against a variety of targets in the

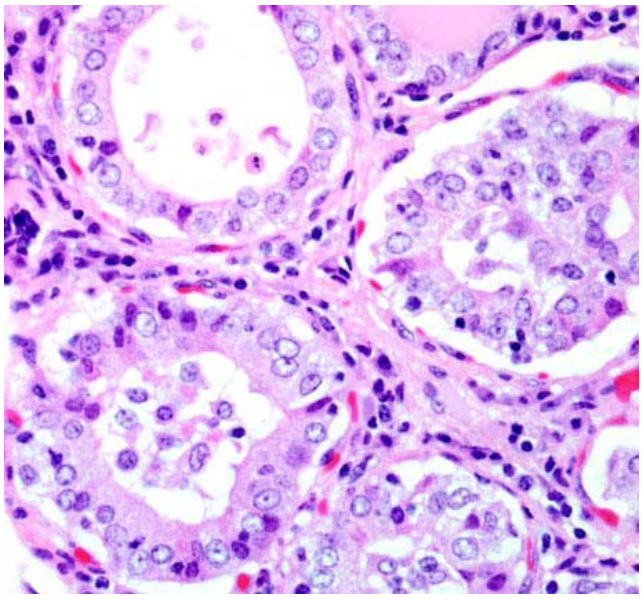

4-2 Thyroid gland, African green monkey. Multifocally thyroid follicles are lined by hypertrophic columnar epithelium with abundant, lightly eosinophilic, finely granular cytoplasm and often follicular lumina are devoid of colloid and contain histiocytes, lymphocytes and plasma cells. (HE 400X).

---

thyroid. Autoantibodies in dogs are most commonly directed against thyroglobulin or against thyroperoxidase or other microsomal antigens; less commonly autoantigens are directed against TSH receptors, a nuclear antigen, or a second colloid antigen from thyroid follicular cells.(5)

Gross lesions in dogs with lymphocytic thyroiditis vary and include normal sized, enlarged or hypoplastic thyroid glands that may be discolored tan to off white. The classic histologic appearance is of multifocal to diffuse infiltrates of lymphocytes and plasma cells that separate thyroid follicles and may form lymphoid nodules. Follicles are often shrunken and lined by columnar epithelial cells, which may cause nests of C cells to appear more prominent between follicles.(2)

Migration of lymphocytes and plasma cells between follicles causes follicular cells to lose their attachment to the basement membrane, and this leads to sloughing of cells into the lumen of the follicle. Lymphoid cells also migrate into the lumen, and this combination of changes leads to eventual death of the follicle. While the damage to follicles is ongoing, adjacent follicles undergo hypertrophy in an attempt to keep up with demand and in response to increased TSH secretion. Eventually the parenchyma of the thyroid gland is replaced by fibrous connective tissue. At this stage, only scant residual inflammatory cells and small, widely dispersed "end-stage" follicles with a small amount of vacuolated colloid remain.(2)

Contributing institution: Animal Resources Program, Wake Forest University Health Sciences

References:

1. Brent GA: Graves' disease. N Engl J Med 358:2594-605, 2008
2. Capen CC: Endocrine Glands. In: Jubb, Kennedy, and Palmer's Pathology of Domestic Animals, ed. Maxie MG, 5th ed., vol.3, p386. Elsevier Saunders, Philadelphia, USA, 2007
3. Caturegli P, Kimura H, Rocchi R, Rose NR: Autoimmune thyroid diseases. Curr Opin Rheumatol 19 (1):44-8, 2007
4.Guzman RE, Radi ZA: Chronic lymphocytic thyroiditis in a cynomolgus monkey (Macaca fascicularis). Tox Pathol 35:296-299, 2007
5. La Perle KM D, Capen C C: Endocrine system. In: Pathologic Basis of Veterinary Disease, ed McGavinMD, Zachary JF, 4th ed., pp.722. Mosby Elsevier, St. Louis, MO 2007
6. Maitra A, Abbas AK: The Endocrine System. In: Robbins and Cotran Pathologic Basis of Disease, ed. Kumar V, Abbas AK, Fausto N, 7th ed., pp1169-73. Elsevier Saunders, Philadelphia, USA, 2005
7. Stockigt J: Assessment of thyroid function: Towards an integrated laboratory – clinical approach. Clin Biochem Rev 24:110-23, 2003
8. Wang SH, Baker JR: The role of apoptosis in thyroid autoimmunity. Thyroid 17(10):975-9, 2007

Notes: